

1 **Revised Manuscript**

2

3 **Marine cements reveal the structure of an anoxic, ferruginous Neoproterozoic ocean**

4

5 **Ashleigh v.S Hood^{1*} and Malcolm W. Wallace¹**

6

7 ¹ *School of Earth Sciences, University of Melbourne, Parkville, VIC, 3010, Australia*

8 ** Corresponding Author (email: ashleigh.hood@student.unimelb.edu.au)*

9

10 Running title: Cements reveal Neoproterozoic ocean structure

11

12 Text: 3007 words

13 39 References: 1051 words

14 3 Figures

15 2 Supplementary data files (including three tables; two diagrams and text)

16

17 **Abstract**

18 Neoproterozoic oceans provided the setting for the rise of animals, yet little is known of their
19 chemical composition. Marine carbonates from the Cryogenian Oodnaminta Reef Complex, South
20 Australia, reveal the chemical structure of a Neoproterozoic ocean. Pseudo-depth profiles from shallow- to
21 deep-water reef facies have been constructed from geochemical and sedimentological analysis of marine
22 cements. Evidence suggests that under peritidal oxic/anoxic chemocline, the water column was largely
23 anoxic, strongly ferruginous and had a chemistry profoundly different from modern seawater. These
24 geochemical data suggest early Archean-like conditions for this Late Cryogenian ocean, posing problems
25 for metazoan evolution in extremely anoxic conditions.

26

27 Supplementary material: detailed methods and data tables are available at www.geolsoc.org.uk/SUP00000.

28

29 The slow buildup of oxygen in the ocean-atmosphere system is arguably the most important
30 evolutionary process in Earth history. Oxygenation of the Earth's surface environments probably occurred
31 in two major episodes, the first; the Great Oxidation Event (Bekker et al., 2004) (~2400-2200 Ma), and
32 the second; the Neoproterozoic Oxygenation Event (Och and Shields-Zhou, 2012) (~800-540 Ma). This
33 latter event is implicated in the evolution of animals and other complex organisms during the
34 Neoproterozoic (Canfield et al., 2007). However, oxygenation was not a simple one-way process (e.g.
35 Lyons et al., 2014) and the details of Precambrian ocean chemistry remain poorly understood.

36 Geochemical studies of Cryogenian and Ediacaran marine sediments indicate that there was a large
37 increase in oxygenation of the oceans during the late Neoproterozoic (Canfield et al., 2007; Och and
38 Shields-Zhou, 2012). Shale geochemistry (iron speciation, trace metals, rare earth element (REE) and
39 several isotope systems) has been the main tool used to constrain Neoproterozoic ocean redox to date. But
40 there are a number of complications in using shales as paleoceanographic proxies. While sediments may
41 record ocean redox conditions, it is often difficult to distinguish between water-mass chemistry and pore-
42 water chemistry, and even more difficult to constrain chemical depth gradients (Piper and Calvert, 2009).
43 Furthermore, deciphering seawater signatures from detrital contamination is problematic. Marine
44 carbonates, which record the chemistry of the parent seawater via trace element incorporation during
45 precipitation, offer a potentially more direct way of determining ancient ocean chemistry (Webb and
46 Kamber 2000; Kamber and Webb, 2001; 2007; Nothdurft et al., 2004). Carbonate microbialites have been
47 successfully used in paleoredox studies (Kamber and Webb, 2007). However, marine cements should
48 record the most reliable marine chemical signatures because they are chemical precipitates that do not
49 incorporate significant detrital material (Nothdurft et al., 2004).

50 A major problem in using carbonates to monitor Neoproterozoic seawater chemistry has been the
51 apparent lack of primary marine precipitates. Marine carbonates of this age are thought to be dominated
52 by an originally aragonitic mineralogy (Hardie, 2003) (which is dolomitised, or converts to calcite during
53 diagenesis and loses its marine chemical signature). However, the recognition of marine dolomite cements
54 from Cryogenian reef complexes (Hood et al., 2011; Hood and Wallace, 2012), provides for the first time,

55 an opportunity to directly analyse unaltered marine precipitates from the Neoproterozoic. Evidence for the
56 primary dolomite mineralogy of these reefal marine cements has been documented in detail and includes
57 both the consistently length-slow nature of the cements and the well-preserved primary growth zonation
58 observed in cathodoluminescent microscopy (Hood and Wallace, 2012; Hood et al., 2011). Additional
59 sedimentological evidence includes the presence of these dolomite marine cements in allochthonous reef
60 blocks in debris flows associated with reef progradation.

61 As these dolomite cements are a product of marine diagenesis in an open reef system and have
62 accordingly precipitated in largely unmodified seawater, they should record the redox state of the water
63 column (e.g. Nothdurft et al., 2004). Geochemical analysis of these dolomite cements reveals the chemical
64 and redox structure of a Cryogenian ocean from the surface to approximately one kilometre depth.

65

66 **Background Geology and Sedimentology**

67 The marine cements analysed in this study are derived from the Late Cryogenian Oodnaminta Reef
68 Complex, consisting of a series of reefal platforms with kilometre-scale relief, in the northern Flinders
69 Ranges, South Australia (Giddings et al., 2009). Although few age constraints exist in this Adelaidean
70 Cryogenian sequence, the upper part of the underlying Sturtian diamictites has been dated at 658Ma using
71 zircon U-Pb dating (Fanning and Link, 2008). The overlying Marinoan glaciation in Australia has been
72 recently dated to terminate at ~636 Ma (Calver et al., 2013). Therefore reef formation is thought to have
73 occurred at approximately 650Ma.

74 The reefs are developed in the dolomitic Balcanoona Formation and generally comprise a
75 relatively flat back-reef platform and a reef margin with two distinct frameworks (Giddings et al., 2009).
76 Shoreward, and laterally equivalent to the reefs, the peritidal facies of the Angepena Formation consist of
77 hematitic dolomites and dolomitic shales (Fromhold and Wallace, 2011). Depositional components of the
78 reefs were originally composed of CaCO₃, but were dolomitised by seawater immediately after their
79 formation (Hood and Wallace, 2012; Hood et al., 2011).

80 We categorize the dolomite marine cements by their depositional facies within the reef complex,
81 which from shallowest to deepest are: 1. Nearshore peritidal (~0-2m water depth); 2. Shallow marine

82 platformal (~0-25m water depth); and 3. deep marine margin (~25m to 1km water depth) (abbreviated as
83 nearshore, shallow and deep respectively). Shallow and deep facies are representative of open marine
84 conditions.

85 'Nearshore' marine cements are hosted by large sheet cavities within hematitic oolitic, intraclastic
86 or micritic dolomites of the Angepena Formation (Fromhold and Wallace, 2011). The presence of
87 abundant teepees and mudcracks within the Angepena Formation provide evidence of a peritidal
88 environment of deposition for this facies. Frequently, ooids from this facies contain hematitic laminae.

89 The 'shallow' marine cements occur in sheet cavities in the platformal facies of the Balcanoona
90 Formation (Giddings et al., 2009; Giddings and Wallace, 2009). These comprise oolitic, intraclastic and
91 micritic dolomites with a complete absence of hematitic lithologies. The shallow marine origin of the
92 facies is indicated by their stratigraphic position within the reef complexes (Giddings et al., 2009;
93 Giddings and Wallace, 2009), the abundance of fenestral and oolitic lithologies, and the presence of
94 stalactitic marine cements (indicating intermittent intertidal conditions).

95 The deep marine margin facies consists of a non-stromatolitic reef framework that underlies a 200-
96 300 m thick stromatolitic framework facies. The stratigraphic position of this facies within the reef
97 complex indicates a deep marine environment (200 to 1000m water depth) (Giddings et al., 2009;
98 Giddings and Wallace, 2009). 'Deep' marine cements occur within growth cavities, and within neptunian
99 dykes in this facies.

100 Marine cements from each of the facies have distinctive optical and cathodoluminescence
101 characteristics. Nearshore cements may have radial-slow, fascicular-slow or radial-slow optical fabrics
102 (Hood and Wallace, 2012), and are generally characterized by well-preserved non- and bright
103 cathodoluminescent zoning. In thin section, nearshore cements may have micro-inclusions of hematite,
104 giving a reddish colour in transmitted light. In contrast, most shallow and deep cements are characterized
105 by radial and fascicular slow fabrics and have weakly dull luminescent zonation.

106

107 **Methods**

108 The petrology and cathodoluminescence character of cements was used as a first step in sample
109 selection. In order to avoid silicate or oxide contamination during analysis, dolomite marine cement
110 analyses were only taken from clean, well preserved samples with sharp, well-preserved
111 cathodoluminescent zonation. Samples with diffuse zonation, areas of recrystallisation, thin carbonate-
112 filled fractures, or non-carbonate inclusions were rejected. Major element concentrations (including Fe
113 and Ca) were analysed using a Cameca SX50 Electron Microprobe at the University of Melbourne with an
114 80s count time, an accelerating voltage of 15kV, and a beam current of 35nA. LA-ICP-MS analyses were
115 carried out on the same samples using a Helex 193 nm ArF excimer laser ablation system connected to an
116 Agilent 7700x quadrupole ICP-MS at the School of Earth Sciences, the University of Melbourne (after
117 Woodhead et al., 2007). An ablation spot size of 93 μm was used, with a laser repetition rate of 10Hz for
118 60 seconds of ablation time. Samples were analysed in blocks of ~ 50 analyses, with a NIST SRM612
119 standard analysed every ~ 7 samples. Data was standardized to Ca (measured by electron microprobe) and
120 reduced by Iolite Software (Paton et al., 2011). The ICP-MS was tuned to give low oxide levels (ThO/Th
121 $< 0.25\%$). Analyses from petrologically unaltered samples were further screened using very stringent
122 geochemical contamination factors (e.g. Th < 0.01 , Al < 10 ppm, total REE < 4 ppm, and coherent REE
123 profiles), tens to hundreds of times lower than previously used for silicate and oxide contamination
124 (Nothdurft et al., 2004; Ling et al., 2013). Detailed methods are available in Supplementary data (**)

125

126 **Geochemical Results and Discussion**

127 *Iron and Manganese*

128 Uncontaminated marine cements record significant chemical variation between near-shore,
129 shallow and deep facies. Electron microprobe analysis reveals high levels of Fe in cements from the
130 shallow and deep cements (mean: 2300 and 3400 ppm respectively) (Fig. 1). In contrast, nearshore
131 cements have low Fe contents, (mean 360 ppm, just above limit of detection). Individual Mn analyses of
132 the nearshore cements reveals that most of this cement has very low levels of Mn (e.g. 10 ppm), with
133 some spots giving very high values (e.g. 1800 ppm). In the shallow and deep cements, spot analyses for
134 Mn have more uniform concentrations that correlate well with Fe.

135 This Fe-Mn behaviour indicates that the nearshore cements were precipitated in oxic/suboxic
136 conditions (where Fe is absent, but Mn may or may not be present) and the shallow and deep cements
137 were precipitated in anoxic conditions (where both Fe and Mn are present)(Barnaby and Rimstidt, 1989).
138 The cathodoluminescent character of the cements, from non- to bright-luminescent in the nearshore
139 cements, and generally dull-luminescent in the shallow and deep cements reinforces this observed
140 geochemical gradient. This interpretation is also consistent with the abundance of hematitic ooidal
141 laminae and other syngedimentary iron oxides in the nearshore facies and their complete absence in the
142 shallow and deep facies. Together, this petrology, sedimentology and geochemistry indicates that with the
143 exception of the uppermost few metres in the nearshore zone, the entire water column was anoxic and
144 strongly ferruginous.

145

146 *Trace metals*

147 The nearshore facies cements show significant enrichment in the elements Cd, Cu, Co, Ni, and U,
148 and depletion in Ba, Cr, Th and total REE, relative to the deeper water facies (Fig. 1). The most extreme
149 enrichments are in Cd and Cu, with average Cu abundance being two orders of magnitude greater than in
150 deeper water facies.

151 Copper and Cd have this behaviour in modern anoxic basins; being enriched in shallow oxic water
152 and strongly depleted in the deeper anoxic water (Calvert and Pedersen, 1993). The disappearance of
153 these metals from the anoxic water in the modern basins is explained by the formation of Cu and Cd
154 sulfides (Jacobs et al., 1985). Thermodynamic modelling shows that sulfide can be present to some degree
155 even in a highly ferruginous ocean because of the formation of aqueous metal-sulfide complexes which
156 buffer total sulfide in the system (Saito et al., 2003). Cu and Cd have such a strong affinity for reduced
157 sulfur that these metals form metals-sulfides in preference to metals like Fe, Mn, Ni, and Co. In particular,
158 Cd has only one valence state and a very strong affinity for sulfide (Saito et al., 2003), indicating that
159 large changes in its concentration between facies represents a change in the presence of dissolved sulphide
160 rather than simply a change in redox.

161 The relative depletion of Ba in the oxic peritidal cements is a corollary for the depletion of Cd in
162 the anoxic facies. Barium has a strong affinity for sulfate, forming the mineral barite. The depletion in Ba
163 in the oxic/suboxic peritidal cements is likely a result of the presence of sulfate in this nearshore
164 environment. The different behaviours of Ba and Cd are therefore reflecting the presence of the
165 sulfate/sulfide interface between the nearshore facies and the more open marine (shallow and deep) facies.
166 The dissolution of barite (and resulting release of Ba) across this interface should account for the high
167 concentrations of Ba in shallow water settings.

168 Similarly, Cr has lowest concentrations in nearshore cements and highest concentrations in
169 shallow water cements. However, Cr will be scavenged by (Fe-) oxides rather than dissolved sulphide
170 (Calvert and Pedersen, 1993), and so its peak concentrations should occur just below the level of Fe-
171 oxide dissolution, reinforcing the presence of a peritidal redoxcline. The distribution of uranium, with
172 highest concentrations in peritidal cements, and negligible concentrations in deeper cements also reflects
173 the presence of this redox interface. Uranium has a soluble form in oxic seawater (i.e. nearshore facies),
174 but will be removed from anoxic waters at the level that Fe-reduction occurs (by shallow marine facies)
175 (Calvert and Pedersen, 1993).

176

177 ***Rare Earth Elements and Yttrium***

178 The nearshore, shallow and deep cements display distinctive rare earth element-Yttrium (REY)
179 profiles (Fig. 2). These elements are more abundant in the anoxic deep-water cements than in the oxic
180 nearshore cements.

181 Rare earth element distributions in modern anoxic basins show similar enrichment in anoxic
182 waters relative to oxic waters because of particle scavenging by Mn/Fe oxides (de Baar et al., 1988;
183 Elderfield et al., 1988). These oxides are precipitated in the upper oxic waters, scavenge REYs, and then
184 sink to be re-dissolved in the deeper anoxic waters releasing the REYs. Consistent with this hypothesis, Fe
185 is strongly correlated with REYs in the shallow and deep cements.

186 The REY profiles for the shallow and deep water cements are dramatically different from
187 Phanerozoic marine signatures, showing little to no light REE depletion, displaying a convex shape

188 (middle REE enriched) and having slight positive Eu and Y/Ho anomalies with a weakly positive Ce
189 anomaly. Ce and Eu anomalies have been calculated as “true” (vs. “apparent”) using the calculations of
190 Bau and Dulski, (1996) and Kamber and Webb, 2001)(See Supplementary data).

191 These characteristics are instead consistent with an anoxic marine chemistry. The lack of light
192 REE depletion is found in anoxic marine basins (Bau and Möller, 1993), while middle REE enriched
193 profiles are found in anoxic ferruginous lakes, hydrothermal oceanic plumes and anoxic diagenetic waters
194 (Johannesson and Zhou, 1999; Sherrell et al., 1999; Haley et al, 2004). Middle REE enrichment has been
195 suggested as being due to anoxic dissolution of iron-oxides, a process which is likely to have occurred in
196 these Cryogenian oceans (Haley et al., 2004). Europium anomalies, also a feature of anoxic marine waters
197 (the strongly positive hydrothermal Eu signature being preserved in anoxic waters) (Bau, 1991) are
198 strongest in deep water cements. The preservation of this high-temperature Eu signature in open marine
199 settings (reefal cements) is reliant on widespread deep-water anoxia from source (i.e. mid-ocean ridge) to
200 continental margin in this fully marine basin. Therefore these positive Eu anomalies are compelling
201 evidence for extensive marine anoxia in Cryogenian oceans. The absence of negative Ce anomalies is
202 similarly a function of anoxic marine chemistry (Ce unlike other trivalent REEs can be oxidized to Ce
203 (IV) in oxic sea water producing negative Ce anomalies) (Bau and Koschinsky, 2009). Significantly,
204 Archean carbonates commonly show similar REY profiles, interpreted as being due to deep water anoxia,
205 but Archean profiles seldom show the middle REE enrichment found in these Cryogenian marine cements
206 (Kamber et al., 2004). This pattern may be the result of an extensive, almost completely anoxic water
207 column in the Cryogenian.

208

209 **Summary and Implications**

210 For the first time, direct marine carbonate precipitates from Neoproterozoic seawater have been
211 geochemically analysed to determine the structure of a Cryogenian ocean. The sum of this geochemical
212 and sedimentological data suggests that these Cryogenian marine cements have precipitated from a
213 severely anoxic and strongly ferruginous water column (except for the very nearshore zone, Fig. 3). This

214 nearshore oxic/suboxic layer may be restricted to coastal waters, where wave action aerates and
215 oxygenates the ocean, or is influenced by oxidised continental waters.

216 Ferruginous deep-ocean conditions have been suggested previously for the Neoproterozoic, largely
217 based on Fe speciation of shales (Canfield et al., 2008; Och and Shields-Zhou, 2012). However, the results
218 from this study provide the first independent evidence of widespread ferruginous conditions during the
219 Cryogenian. Moreover, analysis of these dolomite cements (over a sedimentologically and
220 stratigraphically defined depth range) has enabled the development a detailed redox structure of these
221 Cryogenian oceans. Carbonate geochemistry can thus provide a more refined proxy for
222 palaeoceanographic structure that builds upon the broad foundations developed via shale geochemistry.

223 The enigmatic chemistry and extreme level of anoxia in this Cryogenian ocean requires an
224 explanation. One possibility is that the basin from which these reefal carbonates are derived is not fully
225 open marine (i.e. like the modern Black Sea). However, the geology of the Adelaide Fold Belt is
226 indicative of a fully marine basin, (including the complete absence of evaporites from this Cryogenian
227 succession)(Giddings and Wallace, 2009). The rare earth element profiles, and particularly the prominent
228 positive Eu anomalies in the deep-water cements of this study point to globally anoxic conditions.
229 Moreover, other Neoproterozoic marine sediments, including banded iron formations, globally show
230 chemical evidence for ferruginous and anoxic conditions (review in Och and Shields-Zhou, 2012).

231 Perhaps the reason for the return to Archean-like conditions at this time is linked to the cause of
232 extreme climatic variations in the Neoproterozoic. However, the occurrence of such pervasive ocean
233 anoxia up to ~10 million years after the Sturtian glaciation suggests that large-scale glaciation cannot be
234 the sole cause of these ferruginous conditions. Regardless of the exact cause of this marine anoxia, this
235 carbonate geochemistry has revealed a more complex set of ocean conditions than previously suggested.
236 Significantly, we no longer consider Precambrian ocean oxygenation as a simple two-step process.

237 If this anoxic marine scenario is correct, then the view of Cryogenian oceans being the cradle of
238 metazoan evolution (Erwin et al., 2011) must be viewed in a different light. Early metazoan evolution may
239 have been restricted to oxygenated marine conditions (that developed later in the Ediacaran, or in

240 Cryogenian nearshore conditions) or may have occurred in these anoxic Cryogenian marine settings
241 (Mentel and Martin, 2010).

242

243 We would like to thank two anonymous reviewers for their constructive comments which helped
244 improve this manuscript. The authors acknowledge the Australian Research Council Discovery Project
245 DP130102240 for financial assistance with this research. We would like to thank Doug and Margaret
246 Sprigg for their long-term logistic assistance with fieldwork at Arkaroola.

247

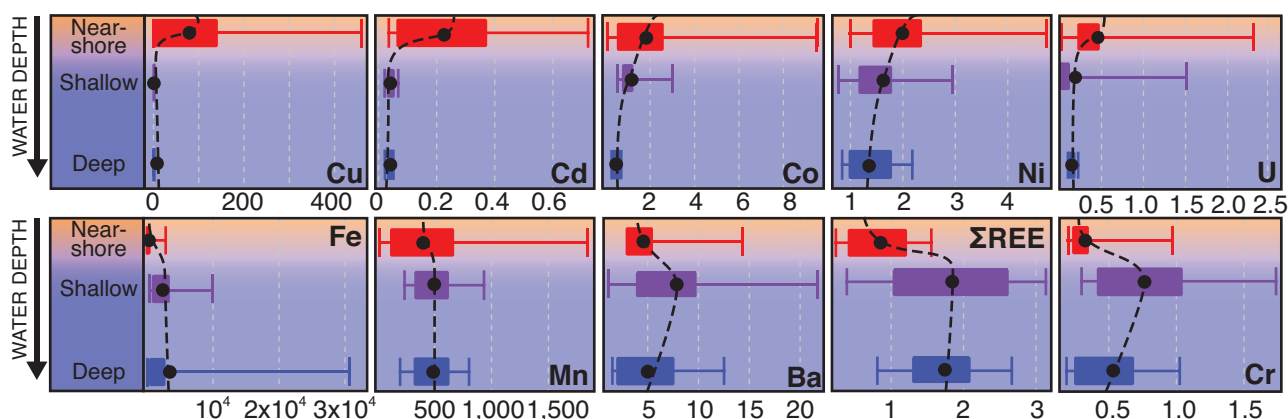
248 **References**

- 249 Barnaby, R.J. and Rimstidt, J.D., 1989. Redox conditions of calcite cementation interpreted from Mn and
250 Fe contents of authigenic calcites. *Geological Society of America Bulletin* **101**, 795-804.
- 251 Bau, M., 1991. Rare-earth element mobility during hydrothermal and metamorphic fluid-rock interaction
252 and the significance of the oxidation state of europium. *Chemical Geology* **93**, 219-230.
- 253 Bau, M. and Koschinsky, A., 2009. Oxidative scavenging of cerium on hydrous Fe oxide: Evidence from
254 the distribution of rare earth elements and yttrium between Fe oxides and Mn oxides in
255 hydrogenetic ferromanganese crusts. *Geochemical Journal* **43**, 37-47.
- 256 Bau, M. and Möller, P., 1993. Rare earth element systematics of the chemically precipitated component in
257 Early Precambrian iron formations and the evolution of the terrestrial atmosphere-hydrosphere-
258 lithosphere system. *Geochimica et Cosmochimica Acta* **57**, 2239-2249.
- 259 Bekker, A., Holland, H.D., Wang, P.-L., Rumble III, D., Stein, H.J., Hannah, J.L., Coetzee, L.L., Beukes,
260 N.L., 2004. Dating the rise of atmospheric oxygen. *Nature* **427**, 117-120.
- 261 Calver, C., Crowley, J., Wingate, M., Evans, D., Raub, T. and Schmitz, M., 2013. Globally synchronous
262 Marinoan deglaciation indicated by U-Pb geochronology of the Cottons Breccia, Tasmania,
263 Australia. *Geology* **41**, 1127-1130.
- 264 Calvert, S. and Pedersen, T., 1993. Geochemistry of recent oxic and anoxic marine sediments:
265 Implications for the geological record. *Marine geology* **113**, 67-88.
- 266 Canfield, D.E., Poulton, S.W. and Narbonne, G.M., 2007. Late-Neoproterozoic deep-ocean oxygenation
267 and the rise of animal life. *Science* **315**, 92-95.
- 268 Canfield, D.E., Poulton, S.W., Knoll, A.H., Narbonne, G.M., Ross, G., Goldberg, T. and Strauss, H., 2008.
269 Ferruginous conditions dominated later Neoproterozoic deep-water chemistry. *Science* **321**, 949-
270 952.
- 271 de Baar, H.J.W., German, C.R., Elderfield, H. and van Gaans, P., 1988. Rare earth element distributions in
272 anoxic waters of the Cariaco Trench. *Geochimica et Cosmochimica Acta* **52**, 1203-1219.
- 273 Elderfield, H., Whitfield, M., Burton, J., Bacon, M. and Liss, P., 1988. The Oceanic Chemistry of the
274 Rare-Earth Elements [and Discussion]. *Philosophical Transactions of the Royal Society of London.*
275 *Series A, Mathematical and Physical Sciences* **325**, 105-126.
- 276 Erwin, D.H. et al., 2011. The Cambrian conundrum: early divergence and later ecological success in the
277 early history of animals. *Science* **334**, 1091-1097.
- 278 Fanning, C.M. and Link, P.K., 2008. Age constraints for the Sturtian Glaciation; data from the Adelaide
279 Geosyncline, South Australia and Pocatello Formation, Idaho, USA. In: S.J. Gallagher and M.W.
280 Wallace (Editors), *Selwyn Symposium 2008 Neoproterozoic extreme climates and the origin of*
281 *early metazoan life*. Geological Society of Australia, Victoria Division, Melbourne, pp. 57.

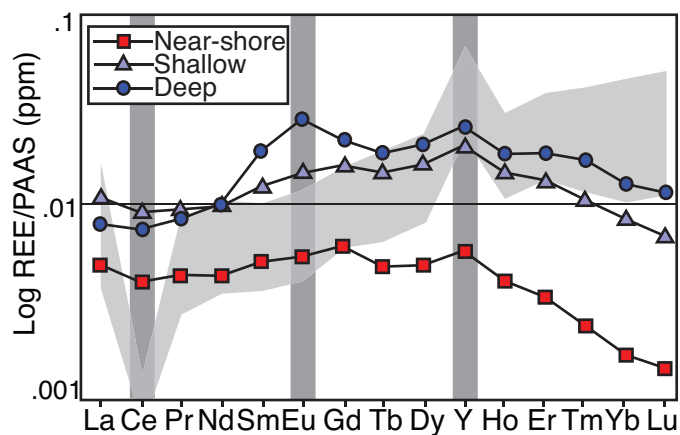
- 282 Fromhold, T.A. and Wallace, M.W., 2011. Nature and significance of the Neoproterozoic Sturtian-
 283 Marinoan Boundary, Northern Adelaide Geosyncline, South Australia. *Australian Journal Of*
 284 *Earth Sciences* **58**, 599-613.
- 285 Giddings, J.A. and Wallace, M.W., 2009. Facies-dependent [δ] ^{13}C variation from a Cryogenian
 286 platform margin, South Australia: Evidence for stratified Neoproterozoic oceans?
 287 *Palaeogeography, Palaeoclimatology, Palaeoecology* **271**, 196-214.
- 288 Giddings, J.A., Wallace, M.W. and Woon, E.M.S., 2009. Interglacial carbonates of the Cryogenian
 289 Umberatana Group, northern Flinders Ranges, South Australia. *Australian Journal Of Earth*
 290 *Sciences* **56**, 907-925.
- 291 Haley, B.A., Klinkhammer, G.P. and McManus, J., 2004. Rare earth elements in pore waters of marine
 292 sediments. *Geochimica et Cosmochimica Acta* **68**, 1265-1279.
- 293 Hardie, L.A., 2003. Secular variations in Precambrian seawater chemistry and the timing of Precambrian
 294 aragonite seas and calcite seas. *Geology* **31**, 785-788.
- 295 Holland, H., 1984. *The chemical evolution of the atmosphere and oceans*. Princeton University Press,
 296 Princeton, 582 pp.
- 297 Hood, A.S. and Wallace, M.W., 2012. Synsedimentary diagenesis in a Cryogenian reef complex:
 298 Ubiquitous marine dolomite precipitation. *Sedimentary Geology* **255–256**, 56–71.
- 299 Hood, A.S., Wallace, M.W. and Drysdale, R.N., 2011. Neoproterozoic aragonite-dolomite seas?
 300 Widespread marine dolomite precipitation in Cryogenian reef complexes. *Geology* **39**, 871-874.
- 301 Jacobs, L., Emerson, S. and Skei, J., 1985. Partitioning and transport of metals across the $\text{O}_2/\text{H}_2\text{S}$ interface
 302 in a permanently anoxic basin: Framvaren Fjord, Norway. *Geochimica et Cosmochimica Acta* **49**,
 303 1433-1444.
- 304 Johannesson, K.H. and Zhou, X., 1999. Origin of middle rare earth element enrichments in acid waters of
 305 a Canadian High Arctic lake. *Geochimica et Cosmochimica Acta* **63**, 153-165.
- 306 Kamber, B.S., 2010. Archean mafic-ultramafic volcanic landmasses and their effect on ocean-atmosphere
 307 chemistry. *Chemical Geology* **274**, 19-28.
- 308 Kamber, B.S., Bolhar, R. and Webb, G.E., 2004. Geochemistry of late Archean stromatolites from
 309 Zimbabwe: evidence for microbial life in restricted epicontinental seas. *Precambrian Research*
 310 **132**, 379-399.
- 311 Kamber, B.S. and Webb, G.E., 2001. The geochemistry of late Archean microbial carbonate:
 312 implications for ocean chemistry and continental erosion history. *Geochimica et Cosmochimica*
 313 *Acta* **65**, 2509-2525.
- 314 Kamber, B.S. and Webb, G.E., 2007. Transition metal abundances in microbial carbonate: a pilot study
 315 based on in situ LA-ICP-MS analysis. *Geobiology* **5**, 375-389.
- 316 Ling, H.-F. et al., 2013. Cerium anomaly variations in Ediacaran-earliest Cambrian carbonates from the
 317 Yangtze Gorges area, South China: Implications for oxygenation of coeval shallow seawater.
 318 *Precambrian Research* **225**, 110-127.
- 319 Lyons, T.W., Reinhard, C.T. and Planavsky, N.J., 2014, The rise of oxygen in Earth's early ocean and
 320 atmosphere. *Nature* **506**, 307-315.
- 321 McLennan, S., 1989. Rare earth elements in sedimentary rocks; influence of provenance and sedimentary
 322 processes. *Reviews in Mineralogy and Geochemistry* **21**, 169-200.
- 323 Mentel, M. and Martin, W., 2010. Anaerobic animals from an ancient, anoxic ecological niche. *BMC*
 324 *Biology* **8**, 32.
- 325 Nothdurft, L.D., Webb, G.E. and Kamber, B.S., 2004. Rare earth element geochemistry of Late Devonian
 326 reefal carbonates, Canning Basin, Western Australia: confirmation of a seawater REE proxy in
 327 ancient limestones. *Geochimica et Cosmochimica Acta* **68**, 263-283.
- 328 Och, L.M. and Shields-Zhou, G.A., 2012. The Neoproterozoic oxygenation event: Environmental
 329 perturbations and biogeochemical cycling. *Earth-Science Reviews* **110**, 26-57.
- 330 Paton, C., Hellstrom, J., Paul, B., Woodhead, J. and Hergt, J., 2011. Iolite: Freeware for the visualisation
 331 and processing of mass spectrometric data. *Journal of Analytical Atomic Spectrometry* **26**, 2508-
 332 2518.
- 333 Piper, D. and Calvert, S., 2009. A marine biogeochemical perspective on black shale deposition. *Earth-*
 334 *Science Reviews* **95**, 63-96.

335 Saito, M.A., Sigman, D.M. and Morel, F.M., 2003. The bioinorganic chemistry of the ancient ocean: the
 336 co-evolution of cyanobacterial metal requirements and biogeochemical cycles at the Archean-
 337 Proterozoic boundary? *Inorganica Chimica Acta* **356**, 308-318.
 338 Sherrell, R.M., Field, M.P. and Ravizza, G., 1999. Uptake and fractionation of rare earth elements on
 339 hydrothermal plume particles at 9 degrees 45 minutes N, East Pacific Rise. *Geochimica et*
 340 *Cosmochimica Acta* **63**, 1709-1722.
 341 Webb, G.E. and Kamber, B.S., 2000. Rare earth elements in Holocene reefal microbialites: a new shallow
 342 seawater proxy. *Geochimica et Cosmochimica Acta* **64**, 1557-1565.
 343 Woodhead, J.D., Hellstrom, J., Hergt, J.M., Greig, A. and Maas, R., 2007. Isotopic and elemental imaging
 344 of geological materials by laser ablation inductively coupled plasma-mass spectrometry.
 345 *Geostandards and Geoanalytical Research* **31**, 331-343.
 346

347 **Figure Captions**



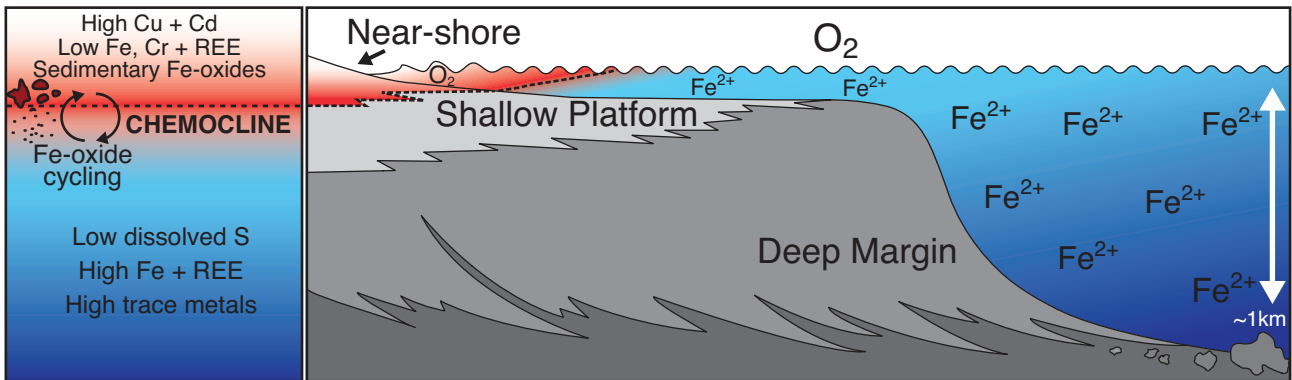
348
 349 1. Pseudo-depth profiles of trace elements in this Cryogenian ocean. Average (black dot), total range of
 350 values (lines) and two sigma range (bar) are provided for nearshore, shallow and deep marine cements.
 351 Based on 55 ‘uncontaminated’ cement analyses.
 352



353
 354 Figure 2. Average rare earth element and yttrium (REY) profiles for nearshore, shallow and deep marine
 355 cements, normalised to the post Archean Australian shale (PAAS; McLennan, 1989). The deep and
 356 shallow profiles display a middle REE enriched pattern with prominent Eu and Y anomalies, consistent

357 with anoxic marine conditions and very different from modern anoxic sea water (Kamber, 2010).

358 Nearshore samples display different profiles with light REE enriched patterns.



359

360 Figure 3. Conceptual model for the chemistry of Cryogenian seawater. The entire open ocean water
361 column is anoxic and ferruginous, while nearshore marine waters are oxic/suboxic, perhaps due to an
362 oxygenated continental influence, or to nearshore wave action in an oxidised atmosphere.

363



Minerva Access is the Institutional Repository of The University of Melbourne

Author/s:

Hood, AVS; Wallace, MW

Title:

Marine cements reveal the structure of an anoxic, ferruginous Neoproterozoic ocean

Date:

2014-11-01

Citation:

Hood, A. V. S. & Wallace, M. W. (2014). Marine cements reveal the structure of an anoxic, ferruginous Neoproterozoic ocean. *Journal of the Geological Society*, 171 (6), pp.741-744. <https://doi.org/10.1144/jgs2013-099>.

Persistent Link:

<http://hdl.handle.net/11343/52114>